Published in final edited form as:
Biochemistry. 2006 March 7; 45(9): 3033–3039.

Functional annotation and kinetic characterization of PhnO from *Salmonella enterica*.

James C. Errey and **John S. Blanchard***
Department of Biochemistry, Albert Einstein College of Medicine, 1300 Morris Park Avenue, Bronx, New York 10461

Abstract

Phosphorus is an essential nutrient for all living organisms. Under conditions of inorganic phosphate starvation, genes from the Pho regulon are induced allowing microorganisms to use phosphonates as a source of phosphorus. The p*hnO gene* was previously annotated as a transcriptional regulator of unknown function due to sequence homology with members of the GCN5-related *N*-acyltransferase family (GNAT). PhnO can now be functionally annotated as an aminoalkylphosphonic acid *N*-acetyltransferase which is able to acetylate a range of aminoalkylphosphonic acids. Studies revealed that PhnO proceeds via an ordered, sequential kinetic mechanism with acetyl-CoA binding first followed by aminoalkylphosphonate. Attack by the amine on the thioester of AcCoA generates the tetrahedral intermediate that collapses to generate the products. The enzyme also requires a divalent metal ion for activity, which is the first example of this requirement for a GNAT family member.

Keywords

Phosphonate metabolism; Enzyme kinetics; Chemical Mechanism; N-acetyltransferases

Phosphorus plays an essential role in the physiology and biochemistry of all living organisms. It is therefore not surprising that microorganisms have evolved sophisticated systems to acquire phosphorus from sources other than inorganic orthophosphate. Under phosphate starvation conditions, when other more readily utilizable forms of phosphate are not present, microorganisms have evolved to utilize more reduced organophosphorus sources, including phosphonates (1). Phosphonates are a class of compounds which contain a carbon-phosphorus (C-P) bond that is exceptionally stable and resistant to chemical hydrolysis, thermal decomposition and photolysis (2). Phosphonates are a naturally occurring class of compound which are present in a number of organisms; e.g. *Tetrahymena* which possesses up to 30% of its membrane lipids in the form of phosphonolipids (3).

Changing the source of phosphorus from orthophosphate to organophosphorus compounds is a tightly regulated process. Under phosphate starvation conditions, genes from the Pho (phosphate starvation) regulon are induced (1). In Gram-negative organisms, like *Salmonella enterica serovar Typhimurium*, the *pho* genes are regulated by a two-component system, which consists of PhoB and PhoR; PhoB binds directly to the *pho* gene promoter whilst PhoR is a P_i sensory histidine protein kinase (4). Two alternative pathways exist for cleavage of the C-P bond: the C-P lyase and the phosphonatase pathways (Scheme 1; (5). *Escherichia coli* carries genes for the reductive C-P lyase pathway (6), whilst *S. enterica* carries genes for the

*Corresponding Author John S. Blanchard, Department of Biochemistry, Albert Einstein College of Medicine, 1300 Morris Park Avenue, Bronx, NY 10461, Tel (718) 430-3096, Fax (718) 430-8565, E-mail address: blanchar@aecom.yu.edu

phosphonatase pathway (7). The C-P lyase pathway has a much broader substrate specificity and is able to cleave alkylphosphonates as well as aminoalkylphosphonates (8,9). In comparison, the phosphonatase pathway has much narrower substrate specificity and acts only on 2-aminoethylphosphonate (10). Mutagenic studies and sequence analysis of the Pho regulon in *Escherichia coli* identified a number of genes involved in phosphonate catabolism designated *phnC* to *phnP* (11,12). PhnC, PhnD, and PhnE were proposed to constitute a phosphonate transporter while PhnG, PhnH, PhnI, PhnJ, PhnK, PhnL, and PhnM were required for catalysis and were proposed to form a membrane-associated carbon-phosphorus (C-P) lyase. PhnN and PhnP were not absolutely required for phosphonate catabolism and were therefore proposed to be accessory proteins for the C-P lyase. PhnF and PhnO were non-essential and were proposed to play regulatory roles because of sequence similarities to other regulatory proteins (11).

In contrast to the *E. coli* Pho regulon which consists of at least 31 co-regulated genes, the *S. enterica* Pho regulon is smaller consisting of only 21 genes (7). The *S. enterica* Phn locus differs from the *E. coli* Phn locus in its size, layout and composition, primarily due to their differing mechanisms of phosphonate catabolism. The *S. enterica* Phn locus is composed of seven genes, designated *phnR* to *phnX* although another cluster containing three genes designated *phnA, phnB* and *phnO* is putatively involved in phosphonate catabolism (Scheme 1; (7,13). Unlike the C-P lyase pathway, the phosphonatase pathway has been extensively mechanistically characterized (7,10,14,15). The initial step in the catabolism of 2-aminoethylphosphonate in *S. enterica* is a PLP-dependent transamination, carried out by 2-aminoethylphosphonate transaminase (the *phnW* gene product;(10). This is followed by a metal-dependent hydrolysis of the C-P bond catalyzed by 2-phosphonoacetaldehyde hydrolase (the *phnX* gene product;(16,17). Interestingly the *phnO* gene is present in both *E. coli* and *S. enterica*, even though they have very different mechanisms of phosphonate catabolism (6,7). Gene knockout studies have shown that the *E. coli phnO* gene product was not required for the catabolism of phosphonates and was presumed to play a regulatory role (11). Furthermore, *phnO* showed significant sequence homology to the GCN5 related *N*-acetyltransferases family (GNAT), of which some members such as the histone acetyltransferases play a regulatory role (18).

In this paper, we describe the cloning, expression, and purification of PhnO from *S. enterica serovar Typhimurium* LT2 and define its functionality as an aminoalkylphosphonic acid *N*-acetyltransferase. We have determined the steady-state kinetic parameters, defined the divalent metal ion dependency and explored the steady-state kinetic mechanism. General acid catalysis is used by the enzyme, and this is likely to be the rate-limiting step as assessed by solvent deuterium kinetic isotope effects.

MATERIAL AND METHODS

All chemicals, acetyl-coenzyme A (CoA), and aminoalkylphosphonic acids were purchased from Sigma-Aldrich Chemical Co or Fisher Scientific. pET-17b(-) plasmid was purchased from Novagen. All restriction enzymes and T4 DNA ligase were obtained from New England Biolabs. *Escherichia coli* strain BL21 (DE3) star cells, PCR primers and the pCR-Blunt plasmid kit was obtained from Invitrogen. *Pfu* DNA polymerase was purchased from Stratagene. DesulfoCoA was synthesized as previously described (19). All divalent metals used in this study were prepared from their respective chloride salt.

General methods

Solution pH values were measured at 25°C with an Accumet model 20 pH meter and Accumet combination electrode standardized at pH 7.0 and 4.0 or 10.0. Protein purification was performed at 4°C using a fast protein liquid chromatography system (Amersham-Pharmacia

Biotech). Spectrophotometric assays were performed using a UVIKON XL double beam UV-vis spectrophotometer (BIO-TEK Instruments). All buffers were passed through Chelex 100 resin (Bio Rad) to remove any divalent metal ions present.

Cloning, expression, and purification of PhnO

The *S. enterica serovar Typhimurium* LT2 gene *phnO* was amplified by PCR using the primers 5-TTTTTCATATGCCAGTCTGTGAATTACGCCA-3 and 5-TTTTTTGAATTCTCACAATGCTTTCGTAAACC-3 from the plasmid template pET-28a (-):*phnO* (generously provided by Sophie Magnet, Albert Einstein College of Medicine), incorporating NdeI and EcoRI restriction endonuclease sites (underlined). The amplified DNA product was ligated into a pCR-Blunt plasmid and transformed into One Shot TOP10 cells. Plasmid DNA isolated from these cells was then digested with NdeI and EcoRI, and the purified insert was ligated into purified plasmid pET-17b(-) previously linearized with the same restriction enzymes, yielding an expression plasmid for *S.enterica phnO*.

The plasmid pET-17b(-):*phnO* was then isolated, sequenced, and used to transform *E. coli* BL21 (DE3) star cells. Transformed cells were grown overnight in 50 ml of LB broth containing 100 μg/ml ampicillin. One-liter cultures were then inoculated, the cells were grown at 37°C to an A_{600} of 0.8. Cells and were then induced by the addition of 0.5 mM isopropyl-β-D-thiogalactopyranoside (IPTG) and left to grow for a further 16 h at 37°C. Soluble expression of the protein was confirmed by sodium dodecyl sulfate polyacrylamide gel electrophoresis (SDS-PAGE).

All protein purification steps were carried out at 4°C. The cell pellet (30 g) was resuspended in 50 ml of buffer A (Buffer A; 20 mM CHES, pH 8.75), containing two tablets of Complete protease inhibitor cocktail (Roche). The cells were disrupted on ice by sonication using a Branson Sonifier 450. The suspension was then centrifuged (10,000 *g* for 30 min) to remove cell debris. The supernatant was filtered using a 0.2 μm Millipore syringe filter and applied to a 140 ml Fast Flow Q-Sepharose anion-exchange column pre-equilibrated with buffer A. The proteins were eluted with a linear, one liter gradient of NaCl (0 to 1 M NaCl) in buffer A volumes at 1 ml/min. Protein was detected with an on-line detector monitoring A_{280}, and column fractions were collected and analyzed by SDS-PAGE. Fractions containing the *ca*. 16 kDa protein were pooled and $(NH_4)_2SO_4$ was added to a final concentration of 1.5 M. After centrifugation to remove insoluble material, the supernatant was applied to a 140 ml Phenyl Sepharose column pre-equilibrated with buffer C (20 mM CHES, pH 8.75, 1.5 M $(NH_4)_2SO_4$). Proteins were eluted with a linear, one liter 1.5 - 0 M $(NH_4)_2SO_4$ gradient at 1 ml/min. The active fractions were pooled and dialyzed extensively against buffer A. The sample was then applied to a 25 ml Mono-Q column anion-exchange column pre-equilibrated with buffer A, and proteins were eluted with a linear 750 ml gradient of NaCl (0 to 1 M NaCl) in buffer A at 1 ml/min. The active fractions were pooled and dialyzed four times against 4 liters of buffer D (Buffer D; 20 mM HEPES 10 mM EDTA, 100 mM $(NH_4)_2SO_4$, pH 8.25) and concentrated using a YM10 Amicon ultrafiltration membrane to a final concentration of 20 mg/ml and stored in 50% glycerol at -20°C.

Determination of protein concentration

The enzyme concentration was determined from $\varepsilon_{280\ nm} = 17780\ M^{-1}\ cm^{-1}$ for native PhnO, and turnover numbers are based on an enzyme monomer. The concentration of enzyme was also determined using the bicinchoninic acid protein assay (Pierce) with bovine serum albumin as a standard, which agreed favorably with the value obtained by A_{280}.

Measurement of Enzyme Activity

Initial velocities for the reaction of PhnO were determined using 4,4′-dithiodipyridine (DTDP) to continuously detect the formation of the product CoA at 324 nm (thiopyridone: ε = 19,800 M^{-1} cm^{-1}) at 25°C A typical reaction mix contained 100 mM HEPES, pH 7.5, 100 mM $(NH_4)_2SO_4$, 200 μM DTDP, 1 mM AcCoA, and 2 mM aminoalkylphosphonate in a final volume of 1 ml. Reactions were initiated by the addition of enzyme, typically 2 nM final concentration. 100 μM Ni^{2+} was typically included because a divalent metal is essential for activity.

Initial Velocity Experiments

Initial velocity kinetic data were fitted using Sigma Plot 2000. The substrate specificity of PhnO was determined at pH 7.5 at 10 different concentrations of the variable substrate and a fixed, saturating concentration of the second substrate and at saturating concentrations of Ni^{2+} [100 μM]. Kinetic constants for acetyl-CoA and other CoA derivatives were determined at fixed saturating concentrations of (*S*)-1-aminoethylphosphonic acid (*S*-1AEP) [3 mM] and Ni^{2+}, whilst kinetic constants for the aminoalkylphosphonates were determined using fixed, saturating concentrations of acetyl-CoA [1 mM] and Ni^{2+}. Kinetic constants for divalent metal ions were determined at fixed saturating concentrations of *S*-1AEP and acetyl-CoA. Individual substrate saturation kinetic data were fitted to Eq. 1

$$v = VA/(A+K) \quad \text{(Eq. 1)}$$

where V is the maximal velocity, *A* is the substrate concentration, and *K* is the Michaelis-Menten constant (K_m). Initial velocity patterns were obtained by measuring the initial rate at five concentrations of each substrate. Eq. 2 was used to fit the intersecting initial velocity pattern,

$$v = VAB/(K_{ia}K_B + K_a B + K_B A + AB) \quad \text{(Eq. 2)}$$

where *A* and *B* are the concentrations of the substrates, K_A and K_B are the Michaelis-Menten constants for the substrates and K_{ia} is the inhibition constant for substrate A.

Dead-end inhibition Studies

Dead-end inhibition patterns were determined by measuring initial velocities (<10% completion) at variable concentrations of one reactant, the second reactant concentration fixed at its K_m value, a fixed, saturating concentration of Ni^{2+} and the inhibitor at several concentrations. Eq. 3 and 4 were used to fit linear, competitive and linear noncompetitive inhibition data, respectively,

$$v = VA/[K(1+I/K_{is}) + A] \quad \text{(Eq. 3)}$$

$$v = VA/[K(1+I/K_{is}) + A(1+I/K_{ii})] \quad \text{(Eq. 4)}$$

where *I* is the inhibitor concentration and K_{is} and K_{ii} are the slope and intercept inhibition constants, respectively.

Dependence of PhnO activity on pH

The pH dependence of the kinetic parameters exhibited by PhnO were determined using *S*-1AEP as the variable substrate. Acetyltransferase activity was monitored from pH 6.75 to 8.5 every ~ 0.5 pH unit using the following buffers: PIPES (pH 6.75-7.35) and HEPES (pH 7.15-8.5). The resulting kinetic data were fitted to Eq.1 to obtain the kinetic parameters; k_{cat} and k_{cat}/K_m. Profiles were generated by plotting the log of k_{cat} or k_{cat}/K_m versus the pH and fitted using Eq. 7 and 8,

$$\log y = \log C/(1+H/K) \quad \text{(Eq. 7)}$$

$$\log y = \log C / \left(1 + H^2/K^2\right) \quad \text{(Eq. 8)}$$

where y is k_{cat} or k_{cat}/K_m, C is the pH-independent value of k_{cat} or k_{cat}/K_m, H is $[H^+]$ and K represents the observed dissociation constant(s) for the ionizing group(s).

Solvent Kinetic Isotope Effects

The solvent kinetic isotope effects on k_{cat} and k_{cat}/K_m were determined by measuring the initial velocities using saturating concentrations of acetyl-CoA and Ni^{2+} whilst varying the concentration of *S*-1AEP in either H_2O or 90% D_2O at pH 8.15. Solvent deuterium kinetic isotope effects were fitted to Eq. 9, where $E_{V/K}$ and E_V are the isotope effects on k_{cat}/K_m -1 and k_{cat} -1, respectively and F_i represents the fraction of isotope

$$v = VA / \left[K\mathrm{A}\left(1 + F_i E_{V/K}\right) + A\left(1 + F_i E_V\right)\right] \quad \text{(Eq. 9)}$$

RESULTS AND DISCUSSION

Cloning, expression and purification of PhnO

To obtain large quantities of PhnO for mechanistic studies, the *phnO* gene was cloned into plasmid pET-17b(-) and expressed in *E. coli* BL21 (DE3) star cells. PhnO was purified using a combination of anion exchange/hydrophobic interaction column chromatographies. These methods were sufficient to achieve a catalytically active protein that was greater than 95% homogeneous (as judged by SDS-PAGE). Approximately 200 mg of purified enzyme was obtained from 30 g of cell paste. Protein electrospray ionization-mass spectrometry was performed on the purified protein, revealing a single species with a molecular mass of 16,499 Da, compared to 16,632 Da expected for full length PhnO, indicating that the N-terminal N-formyl-methionine has been posttranslationally removed. Dynamic light scattering was performed on the protein sample revealing that the protein existed as dimer (data not shown).

Substrate Specificity of PhnO

The substrate specificity of *S. .enterica* PhnO for acyl-CoA derivatives, summarized in Table 1 was determined at fixed saturating concentrations of *S*-1AEP and Ni^{2+}. On the basis of k_{cat}/K_m values and the probability that acetyl-CoA was the likely physiologically relevant substrate, acetyl-CoA was used as the acyl donor in all subsequent experiments. The kinetic parameters of various aminoalkylphosphonic acids determined at fixed saturating concentrations of acetyl-CoA and Ni^{2+} are also summarized in Table 1. The kinetic behavior of the aminoalkylphosphonic acid followed two clear patterns. Increasing the alkyl chain from ethyl to butyl resulted in approximately a 70-fold increase in the K_m values and 13-fold decrease in k_{cat} values, indicating a preference for shorter aminoalkylphosphonic acids. The kinetic data also suggested that the position of the amine group was important with a preference for the 1 position. The k_{cat}/K_m value for *S*-1AEP was 15-fold higher than 2-aminoethyl phosphonic acid, primarily being an effect on the K_m value. The selectivity for the phosphonic acid group was also investigated. Replacement with a carboxyl group, yielding D-alanine, yielded a very poor substrate for which saturation could not be obtained. For D-alanine, only an observed k_{cat}/K_m of 3.0×10^1 M^{-1} sec could be calculated, some 2600-fold lower than the k_{cat}/K_m observed for *S*-1AEP. Mimics of the phosphonate group were also investigated with aminoalkylsulfinic (SO_2H) and aminoalkylsulfonic (SO_3H) acids. Approximately a five-fold decrease of k_{cat}/K_m values were observed with respect to their corresponding phosphonic acid (2-aminoethyl phosphonic acid) and this is primarily a K_m effect.

Metal Ion Requirments

Various divalent metal ions were examined as activators for PhnO. Other enzymes involved in phosphonate catabolism have shown a metal ion dependency, most notably 2-phosphonoacetaldehyde hydrolase (phosphonatase), which requires magnesium for coordination of the phosphonate (17). To investigate whether a tightly-bound metal ion was playing a similar role to that observed in phosphonatase, following the final Mono Q column, PhnO was dialyzed extensively against buffer D in the presence and absence of 10 mM EDTA. Following dialysis with EDTA, PhnO was assayed in the absence of any divalent metal ions. The observed k_{cat}/K_m for *S*-1AEP decreased dramatically after EDTA treatment to 7.2×10^2 M^{-1} sec^{-1}, this being primarily being a K_m effect (Table 2). In contrast when PhnO was extensively dialyzed against buffer alone, the observed k_{cat}/K_m value was 4.6×10^4 M^{-1} sec^{-1}, or half the value determined in the presence of saturating divalent metal ion. This suggests that the enzyme retains half an equivalent of tightly bound divalent metal ion throughout the purification. The metal ion specificity of EDTA-treated PhnO was examined as a function of both the metal ion at fixed, saturating concentrations of acetyl-CoA and *S*-1AEP and the amino phosphonate at fixed concentrations of acetyl-CoA and divalent metal ions (Table 2). The resulting hyperbolic curves (data not shown) were fitted to Eq. 1 to obtain a maximal k_{cat} and K_m values and in the case of the metal ions, the parameter K_{act}, which is defined as the concentration of divalent metal ion required to half saturate the rate. The *S. enterica* PhnO exhibited a preference for Ni^{2+} followed by Mn^{2+} and very poor activity with Mg^{2+}, as evaluated by the k_{cat}/K_{act} values, however it is unclear what the physiologically relevant metal ion activator is and further studies are required.

Kinetic Mechanism

Reactions catalyzed by GNAT acetyltransferases are known to proceed through two distinct mechanisms (18). Only the ESA1 histone acetyltransferase has been shown to proceed via a ping-pong mechanism, with the transfer of the acetyl group from acetyl-CoA to a cysteinyl residue of the enzyme and the subsequent transfer to the ε-amino group of the histone lysine residue (20). The other is a sequential mechanism, where a ternary complex of enzyme, acetyl-CoA, and substrate forms and the acetyl group of acetyl-CoA is directly transferred to a substrate. Reactions catalyzed by all other GNAT superfamily members studied so far, proceed through such a sequential kinetic mechanism (18). The initial velocity patterns were determined using *S*-1AEP and acetyl-CoA at five different concentrations, respectively, and at a fixed, saturating concentration of Ni^{2+}. The resultant double-reciprocal plot was intersecting, diagnostic of a sequential kinetic mechanism in which both substrates must bind to the enzyme before chemistry can take place (Figure 1). Dead-end inhibition experiments were carried out using desulfocoenzyme A *versus* either acetyl-CoA or *S*-1AEP. Desulfocoenzyme A is a coenzyme A analogue that lacks the terminal sulfhydryl of CoA and is a dead-end inhibitor since it forms a non-productive complex with PhnO and the aminophosphonic acid. Desulfocoenzyme A exhibited linear, competitive inhibition *versus* acetyl-CoA (K_{is}: 79 ± 3 μM) and linear, noncompetitive inhibition *versus S*-1AEP (K_{is}: 219 ± 44 μM; K_{ii}: 204 ±: 33 μM). These dead-end inhibition patterns are only compatible with the ordered binding of acetyl-CoA followed by *S*-1AEP, as has been observed with other GNAT acetyltransferases (*18*).

Dependence of pH

pH studies were performed to investigate the ionization behavior of groups responsible for catalysis and binding. The pH depencency of k_{cat} and $k_{cat}/K_{mS\text{-}1AEP}$ were investigated at saturating concentrations of acetyl-CoA and Ni^{2+}. The k_{cat} pH profile revealed the presence a single ionizable group exhibiting a pK value of 8.2 (± 0.1). We ascribed this group to an enzymic group that functions as a general acid involved in protonation of the initially formed thiolate after tetrahedral intermediate collapse. The $k_{cat}/K_{mS\text{-}1AEP}$ profile reveals two groups

with similar pK values of 7.5 (± 0.1) (Figure 2). The two similar pKa's are likely to be ionizable groups from the aminoalkylphosphonate substrate, most likely the amine and the phosphonoxygen groups (both have pK_a values around 7; (21)), both of which are unprotonated when *S*-1AEP binds to the E-acetyl-CoA complex. From these data a chemical mechanism can be proposed where after ordered substrate binding, a tetrahedral intermediate is formed followed by intermediate collapse and protonation of the CoA thiolate (Scheme 2). The exact role of the metal ion is unclear, but could bind to the enzyme and aid in the binding of the aminoalkylphosphonate by coordinating the oxygen's of the phosphonate group in a similar fashion to which 2-phosphonoacetaldehyde hydrolase binds to Mg^{2+} (17). However, we favor a role in which the metal binds to the enzyme, and the aminoalkylphosphonate contributes both the amine and one of the phosphonoxygens atoms as metal ligands, which is supported by the absence of any general base catalysis observed in the k_{cat} pH profile. Preliminary isothermal titration calorimetry data suggest that metals can bind to the free enzyme (data not shown). This could position the amine group of the aminoalkylphosphonate for acetyltransfer and reduce the pK of the amine, making it more nucleophilic for attack on the thioester (such metal complexes of aminoalkylphosphonates have previous been described (22)).

Solvent Kinetic Isotope Effects

Solvent kinetic isotope effects were determined by measuring initial velocities in both H_2O and 90% D_2O. Both acetyl-CoA and *S*-1AEP were investigated as the variable substrate at seven different concentrations, with reactions performed under fixed, saturating concentrations of the other substrate and Ni^{2+}. These experiments were performed at pH 8.15 where both k_{cat} and k_{cat}/K_m are relatively independent of pH. When acetyl-CoA was the variable substrate, a $^{D2O}k_{cat}/K_{acetyl\text{-}CoA}$ value of unity, and a $^{D2O}k_{cat}$ value of 2.2 (± 0.1) were observed, implying that acetyl-CoA binds first, and its dissociation is prevented by *S*-1AEP binding. When *S*-1AEP was the variable substrate, equivalent solvent kinetic isotope effects of 2.2 (± 0.1) were observed on $^{D2O}k_{cat}$ and $^{D2O}k_{cat}/KS_{\text{-}1AEP}$ suggesting that *S*-1AEP is not a "sticky substrate" (Figure 3). These data are in agreement with the dead-end studies that suggested an ordered binding of acetyl-CoA followed by the aminoalkylphosphonate.

A proton inventory experiment was performed by varying the atom fraction of D_2O at saturating concentrations of both *S*-1AEP and acetyl-CoA using Ni^{2+} as the metal activator. Each data point was determined in triplicate, yielding a linear relation between the rate and mole fraction of deuterium (data not shown). The equivalent values of $^{D2O}k_{cat}$ and $^{D2O}k_{cat}/K_{S\text{-}1AEP}$ and the linear proton inventory suggest that a single proton is transferred in a step that is at least partially rate-limiting in the chemical reaction catalyzed by PhnO. On the basis of the k_{cat} pH profile, the most likely single proton transfer is from the enzymic general acid to the thiolate of CoA, formed upon decomposition of the tetrahedral intermediate. In the structures of a number of GNAT-substrate complexes, a suitably positioned tyrosine residue has been ascribed as the general acid (18).

CONCLUDING REMARKS

Although we have demonstrated that PhnO functions as an aminoalkylphosphonic *N*-acetyltransferase, a number of questions still exist. PhnO acetylates a range of aminoalkylphosphonates, including the physiologically relevant 2-aminoethylphosphonic acid. The chemical and kinetic mechanisms proposed are similar to those proposed for other GNAT acetyltransferases, with the sequential binding of acetyl-CoA followed by the binding of the acyl acceptor (the aminoalkylphosphonate), with subsequent formation of the tetrahedral intermediate and product release (23). However, the divalent metal ion activation that was observed is, to date, unique for a GNAT acetyltransferase. It seems likely that the divalent metal ion activation has evolved to play a specific role in aminoalkylphosphonate binding similar to that observed in other enzymes involved in phosphonate catabolism (phosphonatase;

(17). This would also serve to reduce the pK value of the amine and assist in catalysis. The physiological relevance of the PhnO catalyzed reaction is unclear, as acetylation of the amine group would prevent its transamination and subsequent cleavage of the C-P bond. We propose two physiological roles for aminoalkylphosphonate acetylation: storage and protection. When amounts of aminoalkylphosphonates are available in the environment that exceed the organisms phosphate requirements, these phosphonates can be stored in an acetylated form and later used after hydrolysis by a deacetylase. *S*-1AEP is known to have antibacterial properties (24). S-1AEP is a structural analogue of D-alanine, a component of the muramyl-pentapeptide involved in the formation of Gram-negative cross-linked peptidoglycan. *S*-1AEP is a slow onset inhibitor of the *S. enterica* D-alanine:D-alanine ligase, exhibiting a K_i value of 0.5 mM (25). *S*-1AEP is also a slow onset inhibitor of the *Streptococcus faecalis* alanine racemase (26). Thus, PhnO, by acetylating *S*-1AEP, would protect against the deleterious effects of *S*-1AEP as a result of the inhibition of these two key enzymes in peptidoglycan biosynthesis.

Acknowledgement

We thank Sophie Magnet (AECOM) for the generous donation of the *S. enterica* pET-28a(-):*phnO* onstruct. The authors wish to thank Argyrides Argyrou for thoughtful discussions.

This work was supported by NIH Grant AI33696 and AI60899.

ABBREVATIONS

AcCoA, acetyl-Coenzyme A
CHES, 2-(Cyclohexylamino)ethanesulfonic acid
CoA, Coenzyme A
DTDP, 4,4′-dithiodipyridine
EDTA, (Ethylenedinitrilo)tetraacetic acid
GNAT, GCN5-related *N*-acyltransferase
HEPES, N-[2-hydroxyethyl] piperazine-N'-[2-ethanesulfonic acid]
IPTG, Isopropyl-thio-β-D-galactopyranoside
LB, Luria Broth
PCR, polymerase chain reaction
PIPES, Piperazine-1,4-bis(2-ethanesulfonic acid)
S-1AEP, (*S*)-1-aminoethylphosphonic acid
SDS-PAGE, sodium dodecyl sulfate-polyacrylamide gel electrophoresis
TEA, triethanolamine

REFERENCES

1. Vershinina OA, Znamenskaia LV. The Pho regulons of bacteria. Mikrobiologiia 2002;71:581–95. [PubMed: 12449623]
2. Kononova SV, Nesmeyanova MA. Phosphonates and their degradation by microorganisms. Biochemistry (Mosc) 2002;67:184–95. [PubMed: 11952414]
3. Kennedy KE, Thompson GA Jr. Phosphonolipids: localization in surface membranes of *Tetrahymena*. Science 1970;168:989–91. [PubMed: 5441031]
4. Conlin CA, Tan SL, Hu H, Segar T. The apeE gene of *Salmonella enterica serovar Typhimurium* is induced by phosphate limitation and regulated by phoBR. J. Bacteriol 2001;183:1784–6. [PubMed: 11160112]
5. Wanner BL. Molecular genetics of carbon-phosphorus bond cleavage in bacteria. Biodegradation 1994;5:175–84. [PubMed: 7765831]
6. Metcalf WW, Wanner BL. Evidence for a fourteen-gene, *phnC* to *phnP* locus for phosphonate metabolism in *Escherichia coli*. Gene 1993;129:27–32. [PubMed: 8335257]

7. Jiang W, Metcalf WW, Lee KS, Wanner BL. Molecular cloning, mapping, and regulation of Pho regulon genes for phosphonate breakdown by the phosphonatase pathway of *Salmonella typhimurium LT2*. J. Bacteriol 1995;177:6411–21. [PubMed: 7592415]
8. Wackett LP, Shames SL, Venditti CP, Walsh CT. Bacterial carbon-phosphorus lyase: products, rates, and regulation of phosphonic and phosphinic acid metabolism. J. Bacteriol 1987;169:710–7. [PubMed: 3804975]
9. White AK, Metcalf WW. Two C-P lyase operons in *Pseudomonas stutzeri* and their roles in the oxidation of phosphonates, phosphite, and hypophosphite. J. Bacteriol 2004;186:4730–9. [PubMed: 15231805]
10. Kim AD, Baker AS, Dunaway-Mariano D, Metcalf WW, Wanner BL, Martin BM. The 2-aminoethylphosphonate-specific transaminase of the 2-aminoethylphosphonate degradation pathway. J. Bacteriol 2002;184:4134–40. [PubMed: 12107130]
11. Metcalf WW, Wanner BL. Mutational analysis of an *Escherichia coli* fourteen-gene operon for phosphonate degradation, using TnphoA' elements. J. Bacteriol 1993;175:3430–42. [PubMed: 8388873]
12. Metcalf WW, Wanner BL. Involvement of the *Escherichia coli phn* (psiD) gene cluster in assimilation of phosphorus in the form of phosphonates, phosphite, Pi esters, and Pi. J. Bacteriol 1991;173:587–600. [PubMed: 1846145]
13. Kulakova AN, Kulakov LA, Akulenko NV, Ksenzenko VN, Hamilton JT, Quinn JP. Structural and functional analysis of the phosphonoacetate hydrolase (*phnA*) gene region in *Pseudomonas fluorescens* 23F. J. Bacteriol 2001;183:3268–75. [PubMed: 11344133]
14. Dumora C, Marche M, Doignon F, Aigle M, Cassaigne A, Crouzet M. First characterization of the phosphonoacetaldehyde hydrolase gene of *Pseudomonas aeruginosa*. Gene 1997;197:405–12. [PubMed: 9332393]
15. Baker AS, Ciocci MJ, Metcalf WW, Kim J, Babbitt PC, Wanner BL, Martin BM, Dunaway-Mariano D. Insights into the mechanism of catalysis by the P-C bond-cleaving enzyme phosphonoacetaldehyde hydrolase derived from gene sequence analysis and mutagenesis. Biochemistry 1998;37:9305–15. [PubMed: 9649311]
16. Olsen DB, Hepburn TW, Lee SL, Martin BM, Mariano PS, Dunaway-Mariano D. Investigation of the substrate binding and catalytic groups of the P-C bond cleaving enzyme, phosphonoacetaldehyde hydrolase. Arch. Biochem. Biophys 1992;296:144–51. [PubMed: 1605625]
17. Zhang G, Morais MC, Dai J, Zhang W, Dunaway-Mariano D, Allen KN. Investigation of metal ion binding in phosphonoacetaldehyde hydrolase identifies sequence markers for metal-activated enzymes of the HAD enzyme superfamily. Biochemistry 2004;43:4990–7. [PubMed: 15109258]
18. Vetting MW, LP S. d. C. Yu M, Hegde SS, Magnet S, Roderick SL, Blanchard JS. Structure and functions of the GNAT superfamily of acetyltransferases. Arch. Biochem. Biophys 2005;433:212–26. [PubMed: 15581578]
19. Chase JF, Middleton B, Tubbs PK. A coenzyme A analogue, desulpho-coA; preparation and effects on various enzymes. Biochem. Biophys. Res. Commun 1966;23:208–13. [PubMed: 5928913]
20. Yan Y, Harper S, Speicher DW, Marmorstein R. The catalytic mechanism of the ESA1 histone acetyltransferase involves a self-acetylated intermediate. Nat. Struct. Biol 2002;9:862–9. [PubMed: 12368900]
21. Wozniak M, Nicole J, Tridot G. N°701 - Complexes du cuivre (II) et des acides α-aminoalkylphosphoniques: correlation entre acidites, facteurs steriques et pouvoir complexant. Bull. Soc. Chem 1972;11:4445–4452.
22. Song B, Chen D, Bastian M, Martin BR, Sigel H. 155. Metal-Ion-Coordination Properties of a Viral Inhibitor, a Pyrophosphate Analogue, and a Herbicide Metabolite, a Glycinate Analogue: The Solution Properties of the Potentially Five-Membered Chelates Derived from Phosphonoformic acid and (Aminoethyl)phosphonic acid. Helvetica Chem. Acta 1994;77:1738–1756.
23. Draker KA, Northrop DB, Wright GD. Kinetic mechanism of the GCN5-related chromosomal aminoglycoside acetyltransferase AAC(6′)-Ii from *Enterococcus faecium*: evidence of dimer subunit cooperativity. Biochemistry 2003;42:6565–74. [PubMed: 12767240]
24. Badet B, Inagaki K, Soda K, Walsh CT. Time-dependent inhibition of *Bacillus stearothermophilus* alanine racemase by (1-aminoethyl)phosphonate isomers by isomerization to noncovalent slowly

dissociating enzyme-(1-aminoethyl)phosphonate complexes. Biochemistry 1986;25:3275–82. [PubMed: 3730360]

25. Duncan K, Walsh CT. ATP-dependent inactivation and slow binding inhibition of Salmonella typhimurium d-alanine: d -alanine ligase (ADP) by (aminoalkyl)phosphinate and aminophosphonate analogues of d -alanine. Biochemistry 1988;27:3709–14. [PubMed: 3044448]
26. Badet B, Walsh C. Purification of an alanine racemase from *Streptococcus faecalis* and analysis of its inactivation by (1-aminoethyl)phosphonic acid enantiomers. Biochemistry 1985;24:1333–41. [PubMed: 3921052]

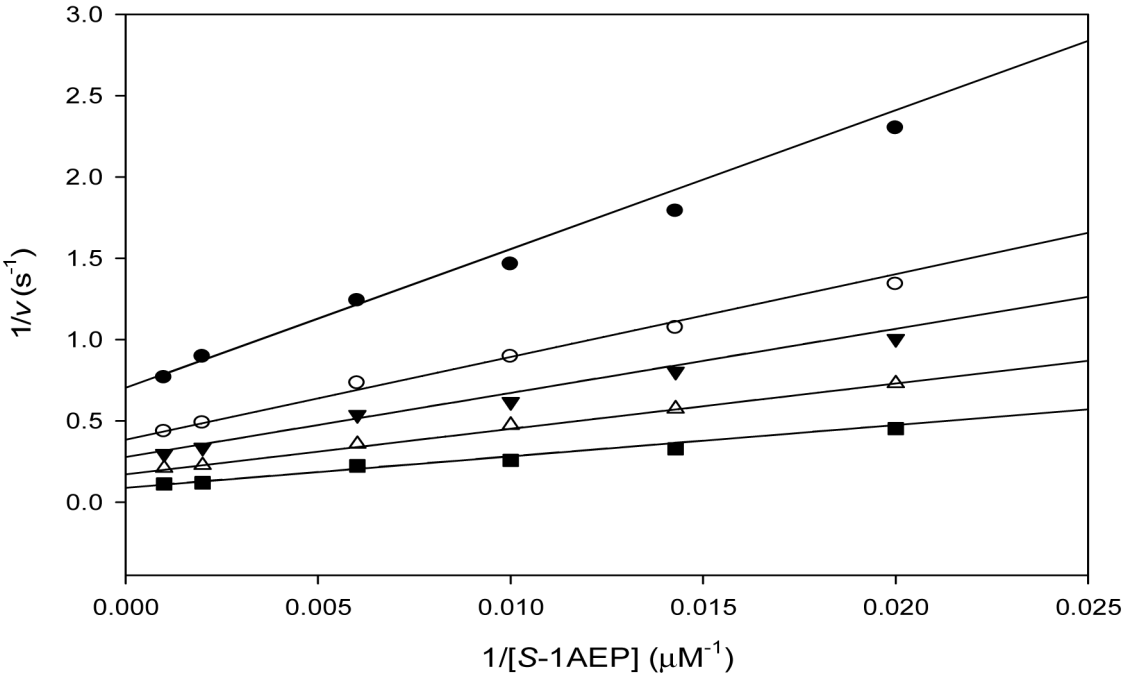

Figure 1.
Double reciprocal plot of initial rate data at varying *S*-1AEP concentrations and fixed concentrations of acetyl-CoA at 10 μM (♀), 20 μM (○), 30 μM (ۍ), 60 μM (→) and 250 μM (†). The pattern of intersecting lines is indicative of a sequential kinetic mechanism.

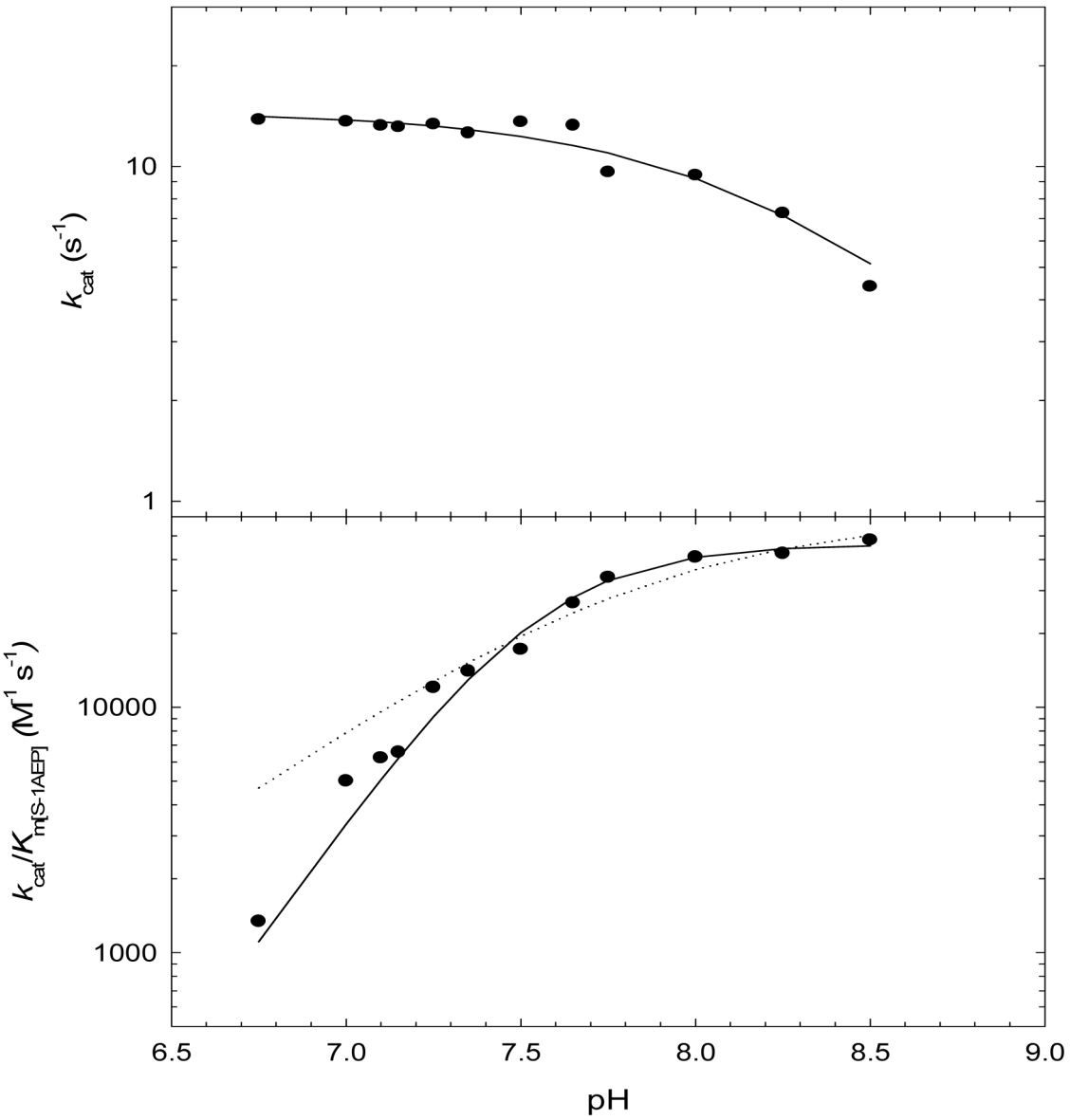

Figure 2.
Dependence of k_{cat} and $k_{cat}/K_{S\text{-}1AEP}$ on pH at saturating levels of acetyl-CoA and Ni^{2+}. The dotted and solid lines are fits to Eqs 7 and 8, respectively. The k_{cat} pH profile revealed the presence a single ionizable group with a pK value of 8.2 (± 0.1). The $k_{cat}/K_{S\text{-}1AEP}$ profile was fit to Eq. 8, which describes the dependence on 2 groups with similar pK values of 7.5 (± 0.1) and Eq. 7, which describes the dependence on 1 group (dotted line).

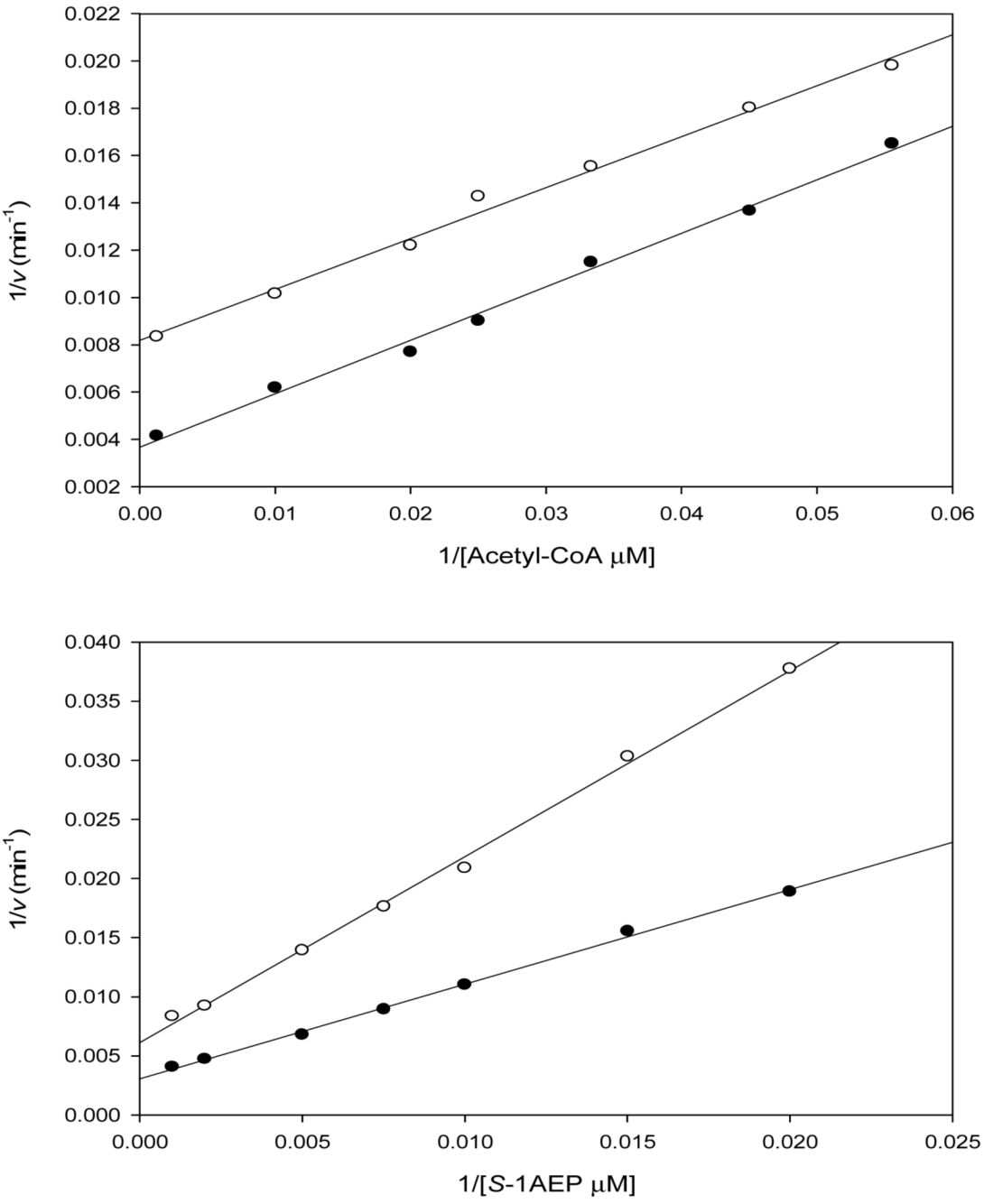

Figure 3.

Reciprocal plots of the solvent kinetic isotope effect determined for PhnO using acetyl-CoA (top panel) or *S*-1AEP (bottom panel) as the variable substrate, in the presence of saturating concentrations of Ni^{2+}. The symbols are the experimentally determined values in H_2O (♀)or 90% D_2O (♋), while the lines are fits of the data to Eq. 9.)

(I) C-P Lyase pathway in *Escherichia coli*

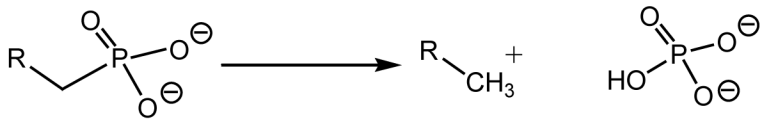

(II) Phophonatase pathway in *Salmonella enterica ssp. typhimurium*

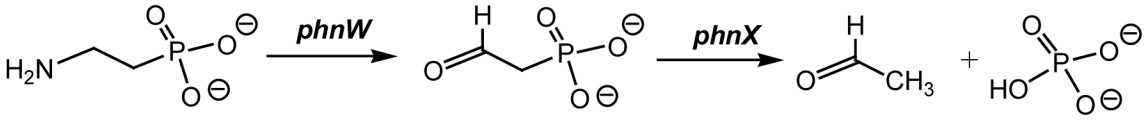

(III) *Salmonella enterica ssp. typhimurium* Phn loci

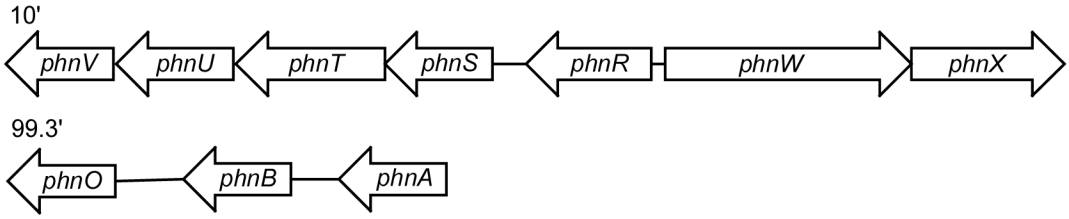

Scheme 1.

Pathways for phosphonate catabolism. (I) The C-P lyase pathway acts on alkylphosphonates as well as aminoalkylphosphonates. (II) The phosphonatase pathway that uses 2-aminoethylphosphonate and cleaves the C-P bond in a two-step transamination and hydrolysis process. (III) The *S. enterica phn* gene locus; *phnR* encodes a putative aminoalkylphosphonate transport repressor, *phnS-V* encode putative aminoalkylphosphonate transport components, *phnW* encodes a 2-aminoethylphosphonate transaminase, *phnX* encodes a 2-phosphonoacetaldehyde hydrolase, *phnA* encodes a putative phosphonoacetate hydrolase, *phnB* encodes a putative phosphonoacetate transporter, *phnO* encodes an aminoalkylphosphonic *N*-acetyltransferase.

I) Kinetic Mechanism

II) Chemical Mechanism

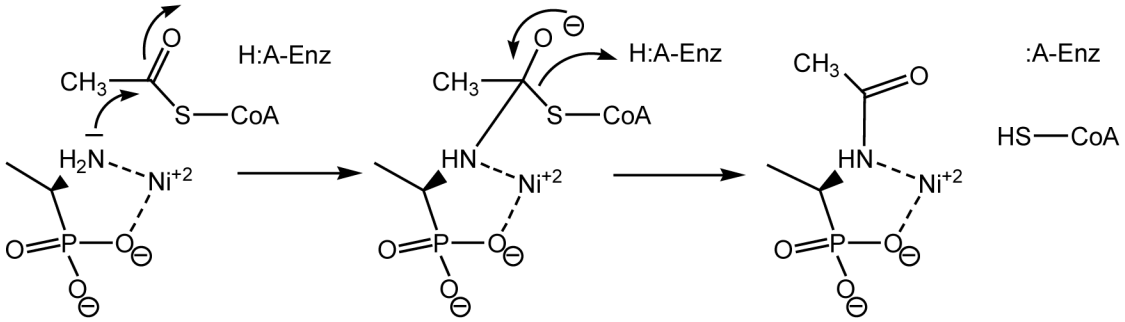

Scheme 2.
Proposed kinetic and chemical mechanisms for aminophosphonate *N*-acetylation by PhnO

Table 1

Kinetic parameters for PhnO with various acyl-CoAs and aminoalkylphosphonates. A) Values for acyl-CoA's were determined at a fixed, saturating concentration of (*S*)-1-aminoethylphosphonic acid. B) Values for aminoalkylphosphonates, and analogs, were determined at a fixed, saturating concentration of AcCoA. NS: not a substrate

Compound	K_m (mM)	k_{cat} (s^{-1})	k_{cat}/K_m (M^{-1} s^{-1})
A			
Acetyl-CoA	0.06 ± 0.01	13.1 ± 0.1	(2.2 ± 0.3) × 10^5
Propionyl-CoA	0.07 ± 0.01	14.7 ± 0.7	(2.1 ± 0.3) × 10^5
Malonyl-CoA	0.05 ± 0.01	0.4 ± 0.1	(8.0 ± 0.6) × 10^3
B			
Aminomethyl phosphonic acid	1.7 ± 0.1	7.0 ± 0.1	(4.1 ± 0.2) × 10^3
2-Aminoethyl phosphonic acid	1.8 ± 0.1	9.0 ± 0.2	(5.0 ± 0.2) × 10^3
3-Aminopropyl phosphonic acid	4.0 ± 0.4	5.4 ± 0.1	(1.4 ± 0.1) × 10^3
4-Aminobutylphosphonic acid	13.0 ± 1.0	0.5 ± 0.1	(3.8 ± 0.4) × 10^1
(*S*)-1-Aminoethylphosphonic acid	0.17 ± 0.01	13.3 ± 0.1	(7.8 ±0.4) × 10^4
(*R*)-1-Aminoethylphosphonic acid	NS		
1-Aminopropyl phosphonic acid	4.1 ± 0.2	7.4 ± 0.1	(1.8 ± 0.1) × 10^3
1-Aminobutyl phosphonic acid	12.5 ± 0.8	1 ± 0.1	(8.0 ± 0.5) × 10^1
D-Alanine			(3.0 ± 0.3) × 10^1
2-Aminoethanesulfonic acid	18.9 ± 0.9	14.8 ± 0.2	(7.8 ± 0.3) × 10^2
2-Aminoethanesulfinic acid	16.4 ± 0.7	20 ± 0.3	(1.2 ± 0.1) × 10^3

Table 2

Kinetic parameters for PhnO with various divalent metal ions. A) Kinetic parameters for *S*-1AEP were determined at a fixed, saturating concentration of AcCoA and the indicated metal ion. B) Kinetic parameters for divalent metal ion activation at saturating concentrations of *S*-1AEP and AcCoA

A	**$K_{mS\text{-}1AEP}$ (mM)**	**k_{cat} (s^{-1})**	**k_{cat}/k_m (M^{-1} s^{-1})**
Mn^{2+}	0.30 ± 0.02	20.6 ± 0.2	(6.9 ± 0.4) × 10^4
Ni^{2+}	0.17 ± 0.01	13.1 ± 0.1	(8.1 ± 0.3) × 10^4
Co^{2+}	0.28 ± 0.06	10.0 ± 0.4	(3.6 ± 0.7) × 10^4
Mg^{2+}	2.00 ± 0.06	17.0 ± 0.3	(8.5 ± 0.3) × 10^3
EDTA treated	18.00 ± 0.76	13.0 ± 0.3	(7.2 ± 0.3) × 10^2
Non EDTA treated	0.20 ± 0.02	9.2 ± 0.2	(4.6 ± 0.4) × 10^4
B	**K_{act} (μM)**	**k_{cat} (s^{-1})**	**k_{cat}/K_{act} (M^{-1} s^{-1})**
Mn^{2+}	6.8 ± 0.6	18.7 ± 1.1	(2.7 ± 0.3) × 10^6
Ni^{2+}	0.6 ± 0.1	13.0 ± 0.3	(2.2 ± 0.3) × 10^7
Co^{2+}	1.3 ± 0.4	8.9 ± 1.1	(6.8 ± 2.2) × 10^6
Cu^{2+}	15.9 ± 2.4	4.5 ± 0.2	(2.8 ± 0.4) × 10^5
Mg^{2+}	850 ± 63	16.8 ± 0.2	(2.0 ± 0.1) × 10^4